current issues in molecular biology

MDPI

Article

Growth Hormone (GH) Attenuates Oxidative Stress and Preserves Structural Plasticity After Prenatal Hypoxic-Ischemic (HI) Injury in the Embryonic Chicken Pallium

Juan David Olivares-Hernández [1,2], Martha Carranza [1], Valeria A. Urban-Sosa [1], Jerusa E. Balderas-Márquez [1], José Ávila-Mendoza [1], Maricela Luna [1], Carlos G. Martínez-Moreno [1] and Carlos Arámburo [1,*]

[1] Departamento de Neurobiología Celular y Molecular, Instituto de Neurobiología, Campus Juriquilla, Universidad Nacional Autónoma de México, Querétaro 76230, Mexico; juolivares@uv.mx (J.D.O.-H.); macasa@unam.mx (M.C.); valjoe28@hotmail.com (V.A.U.-S.); jerusae.balderasm@hotmail.com (J.E.B.-M.); javila@comunidad.unam.mx (J.Á.-M.); lunam@unam.mx (M.L.); cgmartin@comunidad.unam.mx (C.G.M.-M.)

[2] Facultad de Bioanálisis Campus Veracruz, Universidad Veracruzana, Veracruz 91700, Mexico

* Correspondence: aramburo@unam.mx; Tel.: +52-55-5623-4065; Fax: +52-55-5623-4005

Abstract

Oxidative stress is a crucial mechanism in the pathophysiological response to perinatal hypoxia-ischemia (HI), contributing to structural damage and neural death in the immature brain. Although growth hormone (GH) has shown protective effects in HI injury, its underlying mechanisms remain unclear. This study investigated, in vitro and in vivo, whether GH attenuates oxidative stress and preserves neuronal structure after prenatal HI injury using the embryonic chicken *pallium* as the experimental model. In vitro, pallial cell cultures (ED9) were incubated under HI (5% O_2) in low-glucose medium for 24 h, with or without GH, followed by 24 h of reoxygenation (HI/R). Results showed that GH reduced H_2O_2 production and preserved GSH levels, with a partial recovery of the GSH/GSSG ratio. In vivo, embryos (ED14) received GH and were exposed to hypoxia (12% O_2) for 6 h, followed by reoxygenation. GH decreased lipid and protein oxidation and increased SOD and CAT activities. These effects were associated with reduced AIF and HIF-1α protein levels and with differential modulation of antioxidant genes, restoring *Gpx* and *Nrf2* mRNA levels. Importantly, GH preserved dendritic length, branching complexity, and spine density after HI/R. Overall, these findings identify GH as a modulator of redox balance and neuronal structure after prenatal HI injury.

Keywords: growth hormone; hypoxia-ischemia; oxidative stress; *pallium*; prenatal; antioxidant enzymes; neuroprotection; neural plasticity

Academic Editor: Fabrizio De Luca

Received: 15 October 2026
Revised: 8 November 2026
Accepted: 11 November 2026
Published: 14 November 2026

Copyright: © 2026 by the authors. Licensee MDPI, Basel, Switzerland. This article is an open access article distributed under the terms and conditions of the Creative Commons Attribution (CC BY) license.

1. Introduction

Perinatal hypoxic-ischemic encephalopathy (HIE) is a cause of severe brain injury in newborn infants that encompasses complex molecular, cellular, and physiological changes occurring as a result from asphyxia at or around birth. This oxygen deprivation can lead to premature neonatal death or a variety of morbidities, including cerebral palsy, epilepsy, intellectual disability, and behavioral disorders [1,2]. The inefficacy of actual therapeutic strategies in the neonatal population is closely tethered to the impossibility to

predict the development and extent of brain damage after a perinatal insult in most cases, as well as to the intricate pathophysiology of this important public health problem [3].

Some cellular and molecular mechanisms underlying brain harm caused by hypoxic-ischemic (HI) injury involve pathophysiological processes such as excitotoxicity [4], inflammation [5], apoptosis [6], autophagy [7], and oxidative stress [8], among others, which are accountable for neural death and structural damage in the immature brain after an HI insult [2]. The developing brain is particularly vulnerable to the effects of oxidative stress for several reasons, including (a) high metabolic activity and high oxygen consumption; (b) large populations of immature cells; (c) an elevated concentration of iron (Fe^{2+}); (d) a rich content of polyunsaturated fatty acids; and (e) a low concentration of antioxidant enzymes [9]. These conditions make the fetal brain extremely susceptible to the deleterious effects of reactive oxygen species (ROS) and reactive nitrogen species (RNS) [10,11].

ROS are generally small, short-lived, and highly reactive molecules derived from oxygen [12]. They include free radicals like the superoxide radical anion ($O_2^{\bullet-}$) and the hydroxyl radical ($OH^{\bullet}$), as well as some non-radical derivatives of O_2 such as hydrogen peroxide (H_2O_2) and peroxynitrite/peroxynitrous acid (ONOO−/ONOOH). Under normal conditions, ROS are formed as a natural by-product of cellular aerobic metabolism, and their physiological functions include the regulation of many crucial cellular activities such as cell proliferation and differentiation [13]. However, following an HI insult, excessive concentrations of ROS are produced in the brain by dysregulation in the N-methyl-D-aspartate (NMDA) receptors and an exacerbated synthesis of nitric oxide (NO) [14], which results in an oxidative stress environment. Consequently, elevated levels of ROS inflict significant harm in the cells through damage of nucleic acids (DNA or RNA) [15,16], lipid peroxidation of polyunsaturated fatty acids (PUFA, such as membrane phospholipids) [17], and oxidation of proteins [18], leading to structural and functional cellular changes that may cause oxidative injury, apoptosis and necrosis in neurons, oligodendrocytes and glial cells [19–21].

Growth hormone (GH) has emerged as a novel neuroprotective and regenerative factor, with documented actions across various neural injury paradigms in several vertebrate classes [22–27]. These include both in vitro and in vivo models of HI insult in birds and mammals [28–33]. Our group has previously employed the chicken embryo as a good experimental model to study the effects of prenatal hypoxia on brain development as well as the actions of GH as a neurotrophic factor in the cerebellum, the hippocampus and the *pallium* -the avian equivalent of the mammalian cerebral cortex- in response to HI injury. Thus, in a previous study, we identified that GH exerted an anti-apoptotic effect and promoted neurite outgrowth, cell proliferation and synaptogenesis in brain *pallium* during prenatal HI [32]. However, the precise mechanisms through which GH protects the prenatal brain from the deleterious effects of HI injury remain largely unclear. Considering that the immature brain is highly vulnerable to the adverse impacts of oxidative stress [34], the present study investigated, both in vitro and in vivo, whether GH is able to attenuate oxidative stress and preserve neuronal structural integrity in the embryonic chicken cerebral *pallium* after HI/R injury.

2. Materials and Methods

2.1. Animals

Fertilized White Leghorn chicken eggs (*Gallus gallus domesticus)* were donated by Pilgrim's Pride (Querétaro, Mexico) and maintained in a humidified incubator (IAMEX, Queretaro, Mexico) at 39 °C. Throughout incubation, the eggs were automatically rotated 90° every 50 min. All experimental procedures complied with the Mexican Official Standard NOM-062-ZOO-1999 and the international guidelines established in the Guide for the Care and Use of Laboratory Animals (National Research Council, Washington, DC, USA).

https://doi.org/10.3390/cimb48111219

The experimental protocol was reviewed and approved by the Research Ethics Committee of the Institute of Neurobiology (approval No. 038).

2.2. Primary Pallial Cell Cultures

In accordance with Olivares et al., 2022 [32], on embryonic day 9 (ED9), chick embryos were anesthetized in ovo by cooling on ice for 5 min, followed by euthanasia through decapitation. The brains were rapidly isolated from the developing skulls, and the surrounding meningeal membranes were carefully removed. The telencephalic pallia from both hemispheres were then dissected under a stereomicroscope using a microsurgical blade in ice-cold, calcium- and magnesium-free Hanks' balanced salt solution (HBSS). Pallial tissues collected from six embryos were enzymatically dissociated with 0.02% trypsin–EDTA (Sigma-Aldrich, St. Louis, MO, USA) at 39 °C for 10 min, followed by gentle mechanical dissociation using a glass pipette. Cell viability and concentration were determined using the trypan blue exclusion method and a Neubauer hemocytometer. Subsequently, 1×10^5 cells were seeded into 96-well culture plates (Costar Corning, Corning, NY, USA) or onto 12 mm round glass coverslips precoated with poly-L-lysine (50 µg/mL). Cells were maintained in Neurobasal medium supplemented with 2% B27, GlutaMAX, and 1% penicillin–streptomycin (Gibco, Grand Island, NY, USA) (Nb-B27). Cultures were allowed to stabilize for 3 days at 39 °C in a humidified incubator (Series 3 Water Jacketed, Thermo Fisher Scientific, Waltham, MA, USA) under an atmosphere of 95% air and 5% CO_2.

2.3. Treatments

2.3.1. In Vitro Experiments

In vitro hypoxic-ischemic injury and reoxygenation (HI/R group) conditions were induced by substituting normal Nb-B27 medium for DMEM-Low glucose 1× medium (1 g/L, Gibco, Grand Island, NY, USA), and pallial cell cultures were kept in a humidified hypoxia-controlled incubator (HERAcellVIOS 160i, Thermo Fisher Scientific, Waltham, MA, USA) at 39 °C and 5% CO_2. The incubator was flushed with N_2 until the O_2 concentration reached the preset level of 5%. The system was programmed to automatically regulate N_2 delivery as needed to maintain the O_2 concentration at 5% during the 24 h hypoxic period. Immediately after this treatment, the cell cultures were then exposed to reoxygenation (21% O_2) for another 24 h. This situation was achieved by substituting DMEM-Low glucose medium for Nb-B27 medium and incubating the cultures under normoxic conditions (21% O_2, 5% CO_2) for an additional 24 h. After the HI/R stage, the cell cultures were used for analysis. In the control group, cell cultures were maintained in normal Nb-B27 medium under normoxic conditions (Nx group), whereas the cultures conforming the HI/R + GH group received 10 nM recombinant chicken growth hormone (rcGH; Protein Laboratories Rehovot, Rehovot, Israel) in DMEM-Low glucose medium [30,32]. The treatments were added during hypoxia incubation and were maintained during reoxygenation. Because this paradigm combines reduced oxygen and glucose availability, it mimics some features of ischemia in vitro; the term HI/R is used for consistency with our previous studies [28,29,32].

2.3.2. In Vivo Experiments

In vivo hypoxic-ischemic (HI) injury was induced in chicken embryos at embryonic day 14 (ED14) by exposing fertilized eggs to a hypoxic atmosphere (12% O_2) for 6 h at 39 °C in a humidified incubator (NU-4500E CO_2 incubator, NUAire, Plymouth, MN, USA). Following hypoxic exposure, the eggs were transferred to a humidified incubator under normoxic conditions (21% O_2) for an additional 24 h. All subsequent analyses were performed immediately after the reoxygenation period. In parallel, a separate group of

fertilized eggs was maintained under normoxic conditions (21% O_2) and served as the normoxic control (Nx). The experimental treatment groups were microinjected in ovo with two doses of rcGH (2.25 μg each, diluted in 100 μL of saline solution; HI/R + GH group) or with vehicle (HI/R group), administered into the allantoic sac immediately before the 6 h hypoxic period and immediately after it, at the onset of reoxygenation. Because this paradigm consists of systemic hypoxia followed by reoxygenation, without a direct manipulation of cerebral blood flow, an ischemic component of the injury was not directly demonstrated; the term HI/R is retained for consistency with our previous studies using the same model [28,29,32].

2.3.3. Experimental Design and Sample Size

Embryos were randomly allocated to the Nx, HI/R and HI/R + GH groups. Independent cohorts of embryos were used for each assay: a total of 8 embryos per group were assigned to each biochemical assay (TBARS, protein carbonyls, SOD activity and CAT activity); 4 embryos per group were assigned to RT-qPCR studies; 5 (AIF) and 3 (HIF-1α) embryos per group were assigned to Western blot analysis; and 4 embryos per group were assigned to structural examination with Golgi staining. For morphological analyses, 4 embryos per group were employed; ten neurons were traced per embryo, and their values were averaged, so that the embryo was considered the experimental unit. Differences between the initial and final sample sizes correspond to embryos that did not survive the procedure; the final number of embryos analyzed in each assay is indicated in the corresponding figure legend. For in vitro experiments, each independent experiment was performed with a separate cell suspension obtained from the pooled pallia of six embryos. ROS production was evaluated in three independent experiments performed in duplicate, and GSH/GSSG levels were evaluated in three independent experiments performed in triplicate; technical replicates were averaged within each experiment, and the independent experiment (n = 3) was considered the experimental unit.

2.4. CellROX Green Fluorescent Assay

To visualize ROS levels in live cells, the CellROX green assay (Cat. # C10444, Thermo Fisher Scientific, Waltham, MA, USA) was employed. The pallial cells (2.5 × 10^5 cell/well) were cultured in rounded 12 mm cover glasses coated as previously described [30,31]. After the treatments, the CellROX green reagent was added to the medium at a final concentration of 5 μM and incubated for 30 min at 39 °C in the dark according to the manufacturer's instructions. Then, the medium was removed, and the cells were fixed with 4% paraformaldehyde (PFA) for 20 min. The cover glasses were analyzed with an Olympus BX51 fluorescence microscope (Melville, NY, USA), employing a 40× objective. Images were acquired and reconstructed using FIJI-ImageJ software (National Institutes of Health, Bethesda, MD, USA., https://fiji.sc, accessed on 25 July 2023).

2.5. ROS Assay

Production of hydrogen peroxide (H_2O_2) was measured using the ROS-Glo assay kit (Cat. # G8820, Promega, Southampton, UK). The pallial cells (1 × 10^5 cells/well) were cultured in 96-well plates (Costar Corning, Corning, NY, USA) and treated as previously described [30,31]. ROS-Glo H_2O_2 detection solution was prepared according to the manufacturer's guidelines and added to all experimental wells (1:1). After 20 min at room temperature, luminescence was measured using a VARIOSKAN microplate reader (Thermo Fisher Scientific, Waltham, MA, USA). H_2O_2 concentrations were calculated from a standard curve of H_2O_2 processed in parallel with the samples. Protein content of each well was determined by the Bradford assay (Bio-Rad, Hercules, CA, USA), and results were expressed as nmol of H_2O_2 per mg of protein.

2.6. GSH/GSSG Assay

Total glutathione, reduced glutathione (GSH), oxidized glutathione (GSSG) and the GSH/GSSG ratio were determined using the luminescence-based GSH/GSSG-Glo™ assay (Cat. No. V6611, Promega, Southampton, UK). Pallial cells were seeded in 96-well plates at a density of 1×10^5 cells/well and subjected to the experimental treatments described above. Following treatment, the culture medium was removed, and the cells were lysed using either total glutathione lysis reagent or oxidized glutathione lysis reagent, depending on the parameter being measured. The plates were shaken for 5 min, followed by the addition of Luciferin Generation Reagent. After a 30 min incubation at room temperature (RT), luciferin detection reagent was added, and the plates were allowed to equilibrate for an additional 15 min. Luminescence was subsequently recorded using a Varioskan microplate reader (Thermo Fisher Scientific, Waltham, MA, USA). Reduced GSH levels and the GSH/GSSG ratio were calculated from the corresponding measurements. After subtraction of blank luminescence, reduced GSH was calculated by subtracting the GSSG signal from the total glutathione signal, and the GSH/GSSG ratio was calculated for each well as (total glutathione − GSSG)/(GSSG/2), according to the manufacturer's instructions, since each GSSG molecule yields two GSH molecules in the assay. Values from technical triplicates were averaged within each independent experiment, and the experiment means (n = 3) were used for statistical analysis.

2.7. Lipid Peroxidation (TBARS) Assay

Lipid peroxidation was estimated by measuring thiobarbituric acid reactive substances (TBARS) with a commercial assay kit (Cat. # 10009055, Cayman Chemical, Ann Arbor, MI, USA). The pallial tissues (approximately 25 mg) were collected and homogenized in 250 µL of RIPA buffer (25 mM Tris-HCl, pH 7.6, 150 mM NaCl, 1% Triton X − 100, 1% sodium deoxycholate, 0.1% SDS). The tissue homogenates were centrifuged at 10,000 rpm for 15 min at 4 °C. TBARS levels were measured according to the manufacturer's protocol and expressed as MDA equivalents, using the MDA standard provided with the kit. Absorbance at 530 nm was evaluated in a spectrophotometer (Varioskan Flash, Thermo Fisher Scientific, Waltham, MA, USA).

2.8. Protein Carbonyl Assay

To determine the concentration of protein carbonyls in pallial tissue, we used a commercial Protein Carbonyl Colorimetric Assay Kit (Cat. # 10005020, Cayman Chemical, Ann Arbor, MI, USA). After the treatments, pallial tissues (approximately 250 mg) were collected and homogenized in 1 mL of 2-morpholinoethanesulfonic acid (MES) buffer (pH 6.7). The tissue homogenates were centrifuged at 10,000 rpm for 15 min at 4 °C. The protein carbonyl amount was measured according to the manufacturer's protocol. Absorbance at 360 nm was evaluated in a spectrophotometer (Varioskan Flash, Thermo Fisher Scientific, Waltham, MA, USA).

2.9. Superoxide Dismutase (SOD) and Catalase (CAT) Enzymatic Activities

For the determination of the antioxidant enzyme activities, SOD and CAT were determined using the respective assay kits. After the treatments, pallial tissues (approximately 50 mg) were collected; homogenized in 250 µl of 50 mM potassium phosphate buffer, pH 7.4, containing 1 mM EDTA; and centrifuged at 10,000 rpm for 15 min at 4 °C. The SOD activity was measured in the supernatant of pallial tissue by detecting the superoxide radicals generated by xanthine oxidase using a commercially available kit (Cat. # 706002, Cayman Chemical, Ann Arbor, MI, USA), following the manufacturer's protocol. Absorbance at 360 nm was evaluated in a spectrophotometer (Varioskan Flash, Thermo Fisher Scientific, Waltham, MA, USA). The CAT activity was measured by the

reaction of this enzyme with methanol in the presence of an optimal concentration of H_2O_2 using a commercially available kit (Cat. # 707002 Cayman Chemical, Ann Arbor, MI, USA), following the manufacturer's instructions. Absorbance at 540 nm was evaluated in a spectrophotometer (Varioskan Flash, Thermo Fisher Scientific, Waltham, MA, USA).

2.10. SDS-PAGE and Western Blot Analysis

Pallial tissue samples were homogenized by ultrasonication (GE 130PB, Cole-Parmer, Vernon Hills, IL, USA) in 0.05 M Tris-HCl buffer (pH 9.0) supplemented with a protease inhibitor cocktail (Mini-complete, Roche, Mannheim, Germany). The resulting homogenates were centrifuged at 12,500 rpm for 15 min at 4 °C, and the supernatants were collected for subsequent analysis. Total protein concentrations were quantified using the Bradford assay (Bio-Rad, Hercules, CA, USA). Equal amounts of protein (50 μg per lane) were separated by 12.5% sodium dodecyl sulfate-polyacrylamide gel electrophoresis (SDS-PAGE) and subsequently transferred onto nitrocellulose membranes (Bio-Rad, Hercules, CA, USA). For immunoblotting, membranes were blocked with 5% non-fat dry milk in Tris-buffered saline (TBS) for 2 h, followed by overnight incubation at room temperature (RT) with the corresponding primary antibodies (Table 1) diluted in Tris-buffered saline containing Tween 20 (TTBS). After three consecutive washes with TTBS (10 min each), the membranes were incubated for 2 h with the appropriate horseradish peroxidase (HRP)-conjugated secondary antibodies. Immunoreactive protein bands were detected using an enhanced chemiluminescence (ECL) detection reagent (Amersham-Pharmacia, Buckinghamshire, UK) and visualized on autoradiographic film (Fujifilm, Tokyo, Japan). Membranes were stripped and re-probed with anti-GAPDH as a loading control. Kaleidoscope molecular weight markers (Bio-Rad, Hercules, CA, USA) were used as the reference for molecular mass determination. Films were digitized using an imaging system (Bio-Rad Laboratories, Hercules, CA, USA), and band intensities were quantified by densitometry using Image Lab software (version 6.1; Bio-Rad), with values normalized to GAPDH in the same lane.

Table 1. Antibodies used for Western blot analysis.

Target	Host/Type	Dilution	Source	Cat. No.
HIF-1 α	Rabbit/polyclonal	1:1000	Abcam	Ab2185
AIF	Goat/polyclonal	1:500	Santa Cruz	SC-9416
GAPDH	Rabbit/monoclonal	1:3000	Cell signaling	2118
Rabbit IgG	Goat/HRP conjugated	1:3000	Invitrogen	65-6120
Goat IgG	Rabbit/HRP conjugated	1:3000	Invitrogen	81-1620

2.11. Reverse Transcription Polymerase Chain Reaction (RT-PCR)

Total RNA was isolated from approximately 50 mg of pallial tissue using TRIzol reagent (100 μL; Invitrogen, Waltham, MA, USA), following the manufacturer's instructions. RNA samples were subsequently purified using the Direct-zol RNA purification kit (Zymo Research Corp., Irvine, CA, USA). To eliminate potential genomic DNA contamination, the RNA samples were treated with DNase I (Invitrogen, Waltham, MA, USA) for 15 min at room temperature (RT). Complementary DNA (cDNA) was synthesized from 2 μg of total RNA using 100 U of Moloney murine leukemia virus reverse transcriptase (M-MLV; Promega, Madison, WI, USA), 1 mM dNTPs, 0.5 μg of oligo(dT) primers, and 0.5 μg of random hexamer primers. The reverse transcription reaction was performed at 42 °C for 60 min in a final volume of 40 μL.

2.12. Quantitative PCR (qPCR)

The relative expression levels of the target genes listed in Table 2 were determined by quantitative real-time PCR (qPCR) using an ABI PRISM 7900HT system (Applied Biosystems, Foster City, CA, USA) and Maxima SYBR Green chemistry (Thermo Scientific, Waltham, MA, USA). Each reaction was performed in a final volume of 10 µL, containing 3 µL of diluted cDNA and 0.5 µL of each gene-specific primer (0.5 µM final concentration). Primer sequences were designed to amplify avian transcripts while minimizing potential amplification of contaminating genomic DNA (Table 2). The amplification protocol consisted of an initial denaturation step at 95 °C for 10 min, followed by 40 cycles of denaturation at 95 °C for 15 s, annealing at 60 °C for 30 s, and extension at 72 °C for 30 s. Following amplification, melting curve analysis was performed to assess the specificity of the PCR products. Relative mRNA expression levels were calculated using the comparative threshold cycle (Ct) method ($2^{-\Delta\Delta Ct}$) [35–37].

Table 2. Oligonucleotides used for qPCR.

Target	Primer	Sequence (5′-3′)	Size (bp)	Accession #
Cat	Fwd	TGGTGCTGGCAACCCAATAG	168	NM_001031215.2
	Rev	AAATAGCCAAAGGCACCTGCT		
Gpx	Fwd	ACGGCGCATCTTCCAAAG	73	NM_001277853.3
	Rev	TGTTCCCCCAACCATTTCTC		
Nrf2	Fwd	GCCATTCCCGCGTCCAC	81	NM_001396905.1
	Rev	GTCAATCAAGTTCATGTCCTGAGCG		
Sod1	Fwd	GCGCAGGTGCTCACTTCAAT	76	NM_205064.2
	Rev	AGGTCACCCACGTGCCTATC		
Sod2	Fwd	AGGGGAGCCTAAAGGAGAAT	156	NM_204211.2
	Rev	GCTATCTGTAGACGTCCCTGC		
18S	Fwd	CTCTTTCTCGATTCCGTGGGT	100	M59389
	Rev	TTAGCATGCCAGAGTCTCGT		

Gene symbols are in italics in accordance with the official Guidelines for Nomenclature of Genes, Genetic Markers, Alleles and Mutations.

2.13. Golgi-Cox Staining

Brains were stained using the FD Rapid Golgi Stain commercial kit (FD NeuroTechnologies, Ellicott City, MD, USA), following the manufacturer's instructions. Briefly, brains were placed in the impregnation solution, composed of a mixture of equivalent volumes of solution A (potassium dichromate and mercury chloride) and B (potassium chromate), for 14 days in the dark. After that, the brains were transferred to solution C and allowed to stay there for 48 h at 4 °C. Coronal sections (100 µm thick) from *pallium* were obtained using a vibratome. The sections were collected and treated for 10 min at room temperature with a mixture of 1 part solution D, 1 part solution E, and 2 parts bidistilled water. Sections were then rinsed with distilled water and mounted using Permount.

2.14. Sholl Analysis and Dendritic Spine Analysis

Pyramidal neurons of the hyperpallium region (plates A12.6-A7.8) [38] were selected for this study. Neurons were drawn using a camera lucida (Nikon Y-IDT; Tokyo, Japan) attached to a Nikon Eclipse T200 microscope (Nikon, Tokyo, Japan) with a 40× objective. A trained person who was blind to treatment conditions drew a total of 120 neurons. Golgi-Cox-stained pyramidal neurons were identified by their triangle-shaped somas and their numerous dendritic spines. The following criteria were used to select the pyramidal neurons drawn: (1) the location of the cell soma must be in the hyperpallium and within half the thickness of the cut; (2) complete impregnation of the neuron; (3) the presence of

at least three basal dendrites that branched at least once; (4) there should be no changes in the morphology attributed to Golgi-Cox staining. Dendritic morphology was quantified manually by Sholl analysis [39] using a transparent overlay of concentric circles spaced at intervals equivalent to 10 μm at the drawing magnification and centered on the soma. The number of intersections between dendrites and each circle was counted, and total dendritic length was estimated as the total number of intersections multiplied by the 10 μm interval. Dendritic segments were classified by branch order using a centrifugal scheme, in which dendrites originating from the soma were designated as first-order branches and each successive bifurcation defined a higher order. Branches of each order were marked with a different color on the drawings, and their length was estimated from the corresponding number of intersections. Ten neurons were analyzed per embryo, and their values were averaged to obtain a single value per embryo. Spine density was determined by counting spines along 10 μm segments of terminal (last-order) dendrites using a 100× objective.

2.15. Statistical Analysis

Data are expressed as mean ± SEM. For in vitro assays, the independent experiment was considered the experimental unit; for in vivo assays, the embryo was the experimental unit, and morphological data were averaged per embryo before analysis. Differences among the three groups were analyzed by one-way ANOVA, followed by Fisher's protected LSD post hoc test. Branch-order data were analyzed by two-way ANOVA (treatment × branch order), followed by Fisher's LSD test. Unpaired Student's test was used to compare between two groups where appropriate. Analyses were performed with GraphPad Prism (version 9; GraphPad Software, Boston, MA, USA). Values of $p < 0.05$ were considered statistically significant.

3. Results

3.1. GH Reduces ROS in Primary Pallial Cell Cultures Exposed to HI/R Injury

The effect of GH on cellular ROS levels following HI/R injury was initially assessed in vitro using two complementary approaches: the CellROX and the ROS-Glo detection assays (Figure 1). In the first one, which was used only as a qualitative indicator, representative images suggested an apparent increase in green fluorescence intensity after HI/R injury (Figure 1Biv–vi) in comparison with control cultures incubated under normoxic conditions (Figure 1Bi–iii), whereas this increase appeared attenuated in GH-treated cultures (Figure 1Bvii–ix). Using the second approach, H_2O_2 production was quantified as an indicator of oxidative stress, and Figure 1C shows that H_2O_2 concentration increased significantly after HI/R injury (14.34 ± 4.7 nmol/mg protein, $p = 0.005$) in comparison to the normoxia group (1.6 ± 0.06 nmol/mg protein), while the addition of GH to the HI/R-injured cells drastically decreased it (1.51 ± 0.14 nmol/mg protein, $p = 0.005$) to reach control levels.

3.2. Antioxidant Effect of GH in Pallial Cell Cultures Exposed to HI/R Injury

As shown in Figure 2A, HI/R injury reduced total glutathione levels (1.17 ± 0.13 × 10^5 RLU, $p < 0.0001$) in comparison with normoxia condition (2.03 ± 0.12 × 10^5 RLU), whereas GH treatment partially reversed such effect and significantly increased them (1.69 ± 0.09 × 10^5 RLU, $p = 0.004$). Similarly, GSH decreased after HI/R injury (0.78 ± 0.16 × 10^5 RLU vs. 1.74 ± 0.10 × 10^5 RLU in normoxia, $p < 0.0001$) and was significantly higher in GH-treated cultures (1.30 ± 0.11 × 10^5 RLU, $p = 0.001$ vs. HI/R; Figure 2B). In contrast, the cultures exposed to HI/R-injury underwent an increase in GSSG levels (0.4 ± 0.01 × 10^5 RLU, $p = 0.02$; Figure 2C) as compared with the normoxic controls (0.29 ± 0.04 × 10^5 RLU) but

showed no significant difference with the GH treatment group ($0.39 \pm 0.02 \times 10^5$ RLU). On the other hand, the cultures subjected to HI/R injury experienced a strong decrease in the GSH/GSSG ratio (3.87 ± 0.8, $p < 0.0001$; Figure 2D) as compared with the normoxic group (13.09 ± 1.37), whereas the administration of GH induced a partial but significant recovery in the GSH/GSSG ratio in the injured cells (6.78 ± 0.80, $p = 0.01$), although the ratio remained significantly lower than that observed under normoxic conditions ($p = 0.005$).

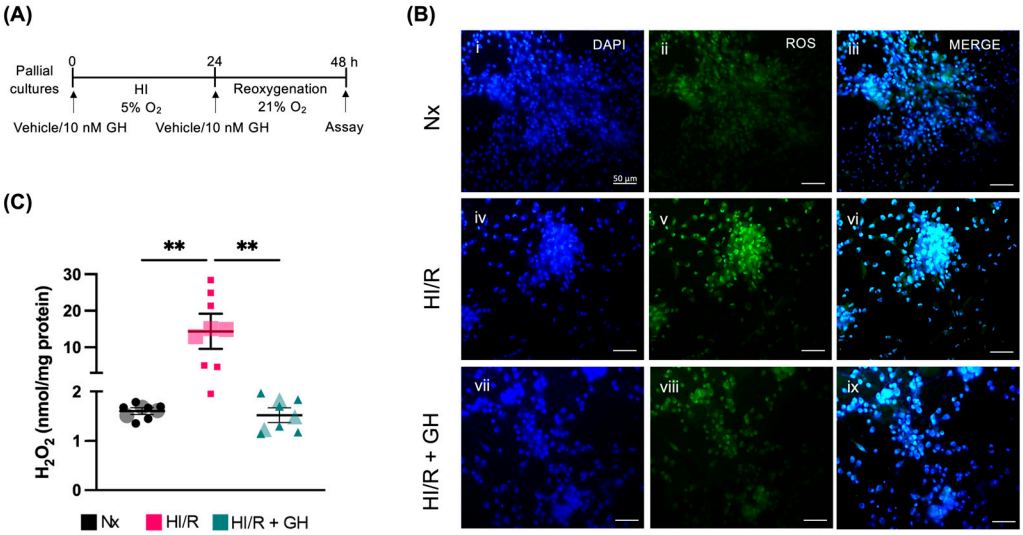


Figure 1. Effect of GH upon generation of ROS after an HI/R injury in embryonic pallial cell cultures. (**A**) Schematic representation of treatments and time course for the in vitro experiment. (**B**) Representative images of pallial cells stained with DAPI (blue) and CellROX (green) and merged images for each experimental condition (qualitative assessment): (**i–iii**) normoxia, (**iv–vi**) HI/R, (**vii–ix**) HI/R + GH. Scale bar: 50 µm. (**C**) H_2O_2 generation was examined using ROS-Glo detection assay. Small symbols represent individual wells (technical duplicates), and large symbols represent the mean of each independent experiment. Horizontal lines show mean ± SEM of the three experiment means ($n = 3$), on which statistical analysis was performed. Asterisks show multiple comparisons among groups, ** $p < 0.01$, determined by one-way ANOVA with Fisher's protected LSD as post hoc test.

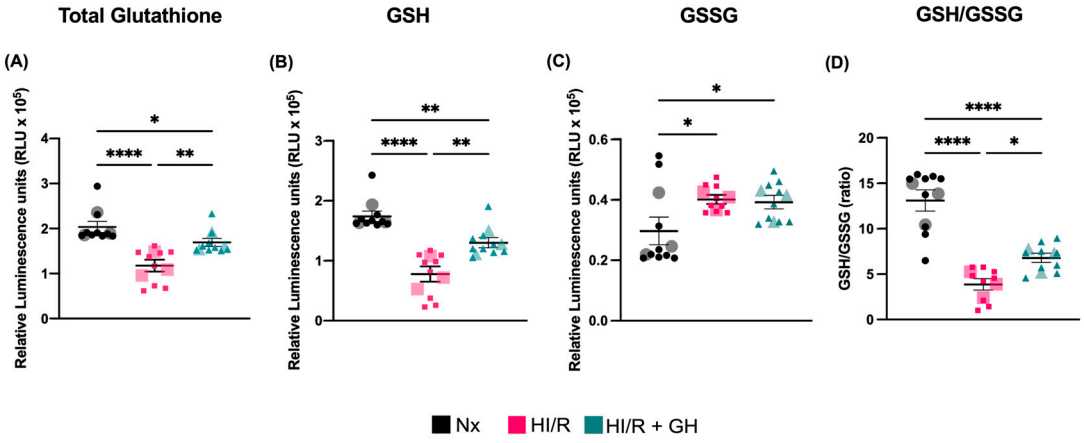


Figure 2. Effect of GH on glutathione levels in embryonic pallial cell cultures after a hypoxic-ischemic and reoxygenation (HI/R) injury**.** Total glutathione (**A**), reduced GSH (**B**), GSSG (**C**), and GSH/GSSG ratio (**D**) were evaluated in pallial cell cultures using GSH/GSSG-Glo assay. Reduced GSH was calculated as total glutathione minus GSSG, and the GSH/GSSG ratio was calculated as

(total glutathione − GSSG)/(GSSG/2). Small symbols represent individual wells (technical triplicates), and large symbols represent the mean of each independent experiment. Horizontal lines show mean ± SEM of the three experiment means (n = 3), on which statistical analysis was performed. Asterisks show multiple comparisons among groups, * $p < 0.05$, ** $p < 0.01$, **** $p < 0.0001$, determined by one-way ANOVA with Fisher' protected LSD as post hoc test.

3.3. GH Reduces Oxidative Damage and Prevents Lipid Peroxidation and Protein Carbonylation in an In Vivo Model of HI/R

Figure 3 shows the effects of oxidative damage and GH treatment upon lipid peroxidation and protein carbonylation in the pallial tissue obtained from the in vivo chick embryo model. As shown in Figure 3B, TBARS levels, expressed as MDA equivalents, revealed a significant increase in lipoperoxidation in the HI/R group (3.28 ± 1.02 nmol/mg protein, $p = 0.02$) compared with normoxia (1.18 ± 0.20 nmol/mg protein). This deleterious effect was prevented in the HI/R + GH group (1.28± 0.21 nmol/mg protein; $p = 0.03$). Likewise, protein carbonyl content was drastically increased after HI/R injury (1.41 ± 0.12 nmol/mg protein, $p = 0.02$; Figure 3C) in comparison with the normoxic group (1.05 ± 0.04 nmol/mg protein). GH treatment significantly reversed HI/R-induced protein oxidation (1.0 ± 0.11 nmol/mg protein, $p = 0.008$), restoring levels comparable to those observed under normoxic conditions.

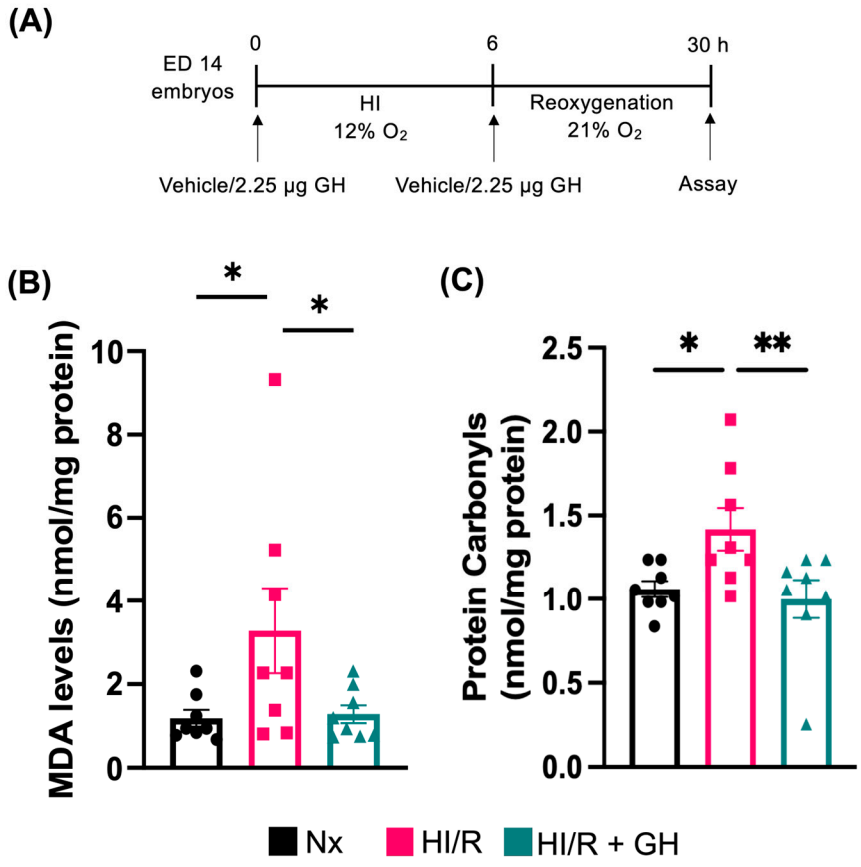


Figure 3. Effect of GH upon oxidation of lipids and proteins in embryonic chicken *pallium* exposed to a hypoxic-ischemic and reoxygenation (HI/R) injury. (**A**) Treatments and time course schematic representation of in vivo experiment. (**B**) TBARS levels, expressed as MDA equivalents, and (**C**) protein carbonyl levels were determined in the embryonic chicken *pallium*. Bars represent mean ± SEM. (**B**,**C**) $n = 8$ embryos per group. Asterisks show multiple comparisons among groups, * $p < 0.05$, ** $p < 0.01$, determined by one-way ANOVA with Fisher' protected LSD as post hoc test.

https://doi.org/10.3390/cimb48111219

3.4. GH Effects on SOD and CAT Activities

The antioxidant effect of GH was also evaluated by measuring SOD and CAT activities in the embryonic pallial tissue. As shown in Figure 4A, exposure to HI/R injury significantly reduced SOD activity (0.28 ± 0.01 U/mg protein, $p = 0.0003$) in comparison to the normoxic control (0.38 ± 0.01 U/mg protein). However, GH administration during HI/R increased SOD activity (0.33 ± 0.01 U/mg protein, $p = 0.03$), partially restoring enzyme levels. Similarly, Figure 4B shows that HI/R injury significantly reduced CAT activity (0.52 ± 0.04 nmol/min/mg protein, $p = 0.03$); in contrast, GH treatment during HI/R injury markedly increased CAT activity (0.96 ± 0.08 nmol/min/mg protein, $p = 0.0003$), exceeding normoxic levels (0.7 ± 0.05 nmol/min/mg protein, $p < 0.05$).

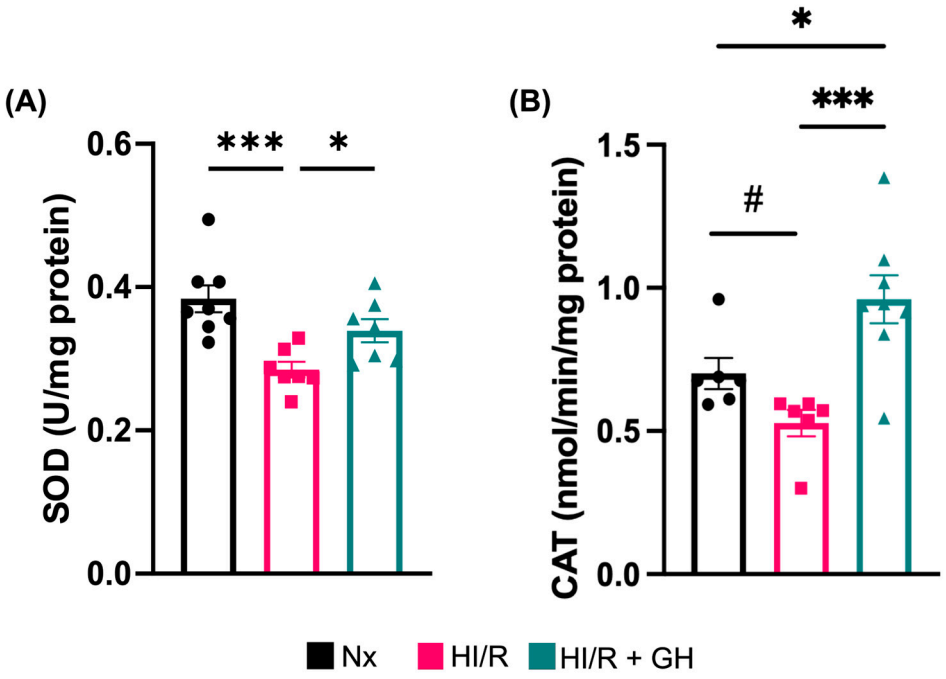


Figure 4. Effect of GH upon antioxidant enzymatic activity in embryonic chicken *pallium* exposed to a hypoxic-ischemic and reoxygenation (HI/R) injury. (**A**) SOD activity and (**B**) CAT activity were measured in the embryonic chicken *pallium*. Bars represent mean ± SEM. (**A**) $n = 8$, 7 and 7 embryos; (**B**) $n = 6$, 6 and 8 embryos for the Nx, HI/R and HI/R + GH groups, respectively. Embryos that did not survive the procedure were excluded. Asterisks show multiple comparisons among groups, * $p < 0.05$, *** $p < 0.001$, determined by one-way ANOVA with Fisher' protected LSD as post hoc test. An unpaired Student's t test was used to compare Nx versus HI/R groups (panel B). # indicates significant differences (# $p < 0.05$).

3.5. GH Regulates Expression of Antioxidant Enzyme Genes After HI/R Injury

Figure 5 shows the effect of HI injury and GH treatment upon the expression of several antioxidant-related genes (*Sod1*, *Sod2*, *Cat*, *Gpx* and *Nrf2*) in the pallial tissue. It was found that *Sod1* and *Sod2* mRNA levels decreased following HI/R injury (0.75-fold and 0.73-fold; Figures 5A and 5B, respectively), although only the reduction in *Sod2* showed statistical significance ($p = 0.04$). In contrast, *Cat* mRNA expression showed a tendency to increase after HI/R injury (1.6-fold; Figure 5C) compared with normoxic controls, without reaching statistical significance ($p = 0.08$). Notably, GH administration during HI/R significantly reduced *Cat* expression (0.7-fold, $p = 0.02$). On the other hand, *Gpx* mRNA expression was significantly reduced following HI/R (0.4-fold, $p = 0.004$; Figure 5D); however, GH treatment during HI/R restored *Gpx* expression to control levels (1-fold, $p = 0.003$).

Likewise, *Nrf2* mRNA expression (Figure 5E) decreased in response to HI/R compared with normoxic controls (0.47-fold, $p = 0.02$) and was significantly upregulated under HI/R + GH condition (1-fold, $p = 0.02$).

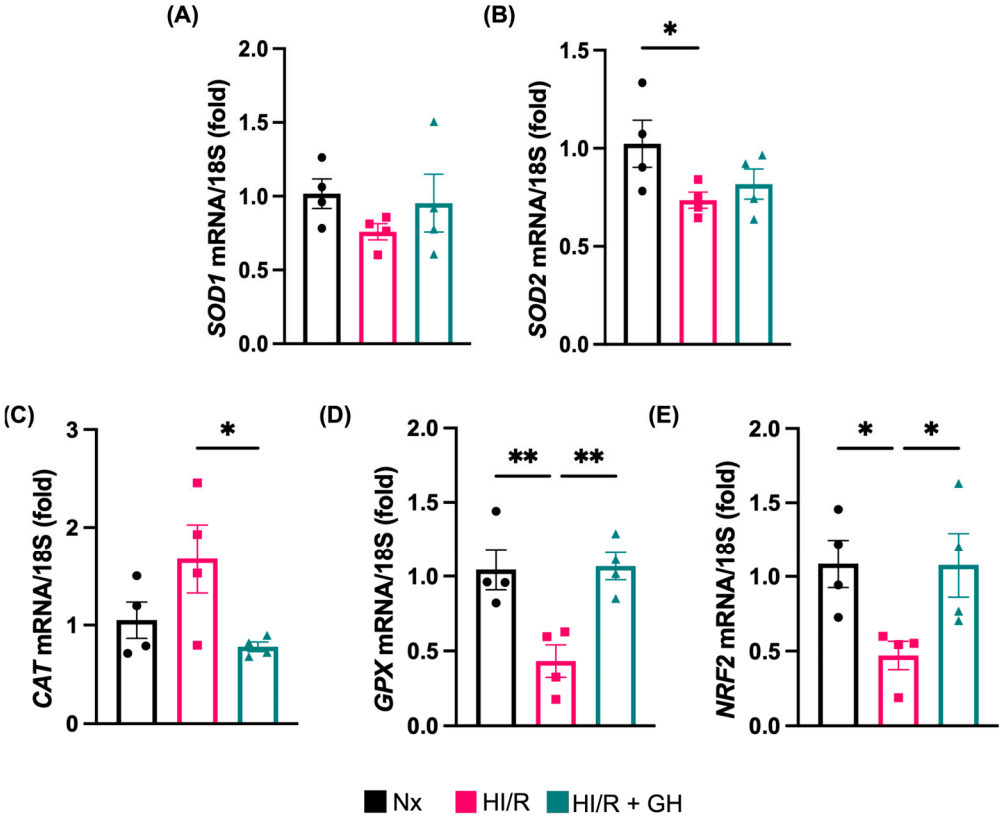


Figure 5. Effects of GH on antioxidant enzyme genes expression after hypoxic-ischemic and reoxygenation (HI/R) injury. Panels show the mRNA expression of (**A**) *Sod1*, (**B**) *Sod2*, (**C**) *Cat*, (**D**) *Gpx* and (**E**) *Nrf2*, as determined by RT-qPCR. Relative mRNA expression values were corrected by the comparative threshold cycle (Ct) method and employing the formula $2^{-\Delta\Delta CT}$. Ribosomal 18S RNA was used as the housekeeping gene. Bars represent mean ± SEM; $n = 4$ embryos per group. Asterisks show multiple comparisons among groups, * $p < 0.05$, ** $p < 0.01$, determined by one-way ANOVA with Fisher's protected LSD as post hoc test.

3.6. Effects of GH upon the Expression of Apoptosis Inducing Factor (AIF) and Hypoxia-Inducible Factor 1-Alpha (HIF-1α) After HI/R Injury

Figure 6 shows the effects of normoxic, HI/R, and HI/R + GH treatments on AIF and HIF-1α protein levels in pallial tissue, as analyzed by Western blot (WB). As described in Figure 6A, AIF immunoreactivity (AIF-IR) showed a tendency to increase after HI/R injury (113 ± 8.1%, $p = 0.06$) in comparison to the normoxic controls (95.21 ± 5.34%), while the administration of GH during HI/R significantly reduced AIF-IR levels to those observed under normoxia (92.3 ± 5.15%, $p = 0.04$). On the other hand, Figure 6B shows that the HI/R condition significantly increased HIF-1α-IR in the pallial tissue (110.1 ± 0.66%, $p = 0.017$) in comparison to chick embryos maintained under normoxic conditions (100 ± 2.64%). Interestingly, GH treatment reduced HIF-1α-IR to 91.22 ± 2.61% % in the injured group ($p = 0.001$), below normoxic levels ($p = 0.029$).

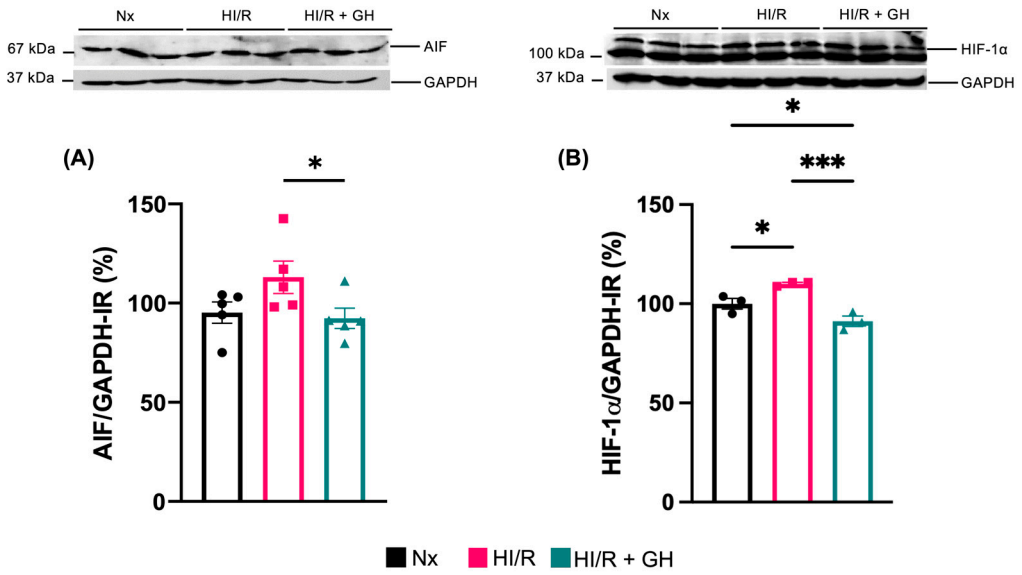


Figure 6. Effects of GH upon expression of AIF and HIF-1α protein levels in the *pallium* of chick embryos exposed to hypoxic-ischemic and reoxygenation (HI/R) injury, as determined by Western blot. (**A**) Densitometric analysis of immunoblots stained for AIF immunoreactivity (AIF-IR). (**B**) Densitometric analysis of immunoblots stained for HIF-1α-IR. The signal of each lane was normalized to the GAPDH signal of the same lane after stripping and re-probing the membrane and expressed as a percentage of the mean of the normoxic (Nx) group. Bars represent mean ± SEM; each lane corresponded to one embryo. (**A**) n = 5 embryos per group; (**B**) n = 3 embryos per group. Full uncropped membranes are shown in Supplementary Figure S1. Asterisks show multiple comparisons among groups, * $p < 0.05$, *** $p < 0.001$, determined by one-way ANOVA with Fisher' protected LSD as post hoc test.

3.7. GH Promotes Structural Plasticity After HI/R Injury

Figure 7 shows the effect of oxidative damage and GH treatment upon several morphometric parameters related to structural plasticity of pallial neurons. Image analysis of Golgi-stained neurons showed that HI/R injury altered neuronal morphology, reducing dendritic length and arborization complexity (Figure 7Aii), compared with neurons from chick embryos maintained under normoxic conditions (Figure 7Ai). In contrast, neurons from GH-treated embryos exhibited a morphology similar to that of normoxic controls, as dendritic length and arborization complexity were restored (Figure 7Aiii). Representative microphotographs of dendritic segments showed that HI/R injury reduced spine number (Figure 7Bii) compared with the normoxic group (Figure 7Bi), whereas neurons from the GH-treated group kept spine number at levels comparable to controls (Figure 7Biii).

Sholl analysis revealed that total dendritic length was significantly reduced after HI/R injury compared to control animals (Nx = 614.5 ± 20.11 μm vs. HI/R = 378.5 μm ± 14.63, $p < 0.0001$; Figure 7C). Interestingly, GH treatment prevented this reduction by increasing the total dendritic length (667.9 ± 29.68 μm, $p < 0.0001$), reaching values comparable to those of normoxic controls. Branch-order analysis showed that HI/R reduced dendritic length mainly at the second, third, and fourth branch orders and that these reductions were prevented by GH ($p < 0.0001$, $p < 0.0001$, and $p < 0.01$, respectively; Figure 7D). Regarding dendritic spine density, spine number was significantly reduced under the HI/R condition compared to normoxia (Nx = 7.4 ± 0.38 spines/10 μm vs. HI/R = 5.8 ± 0.3 spines/10 μm, $p = 0.004$; Figure 7E); in turn, GH administration improved spine density (6.9 ± 0.5 spines/10 μm, $p = 0.04$).

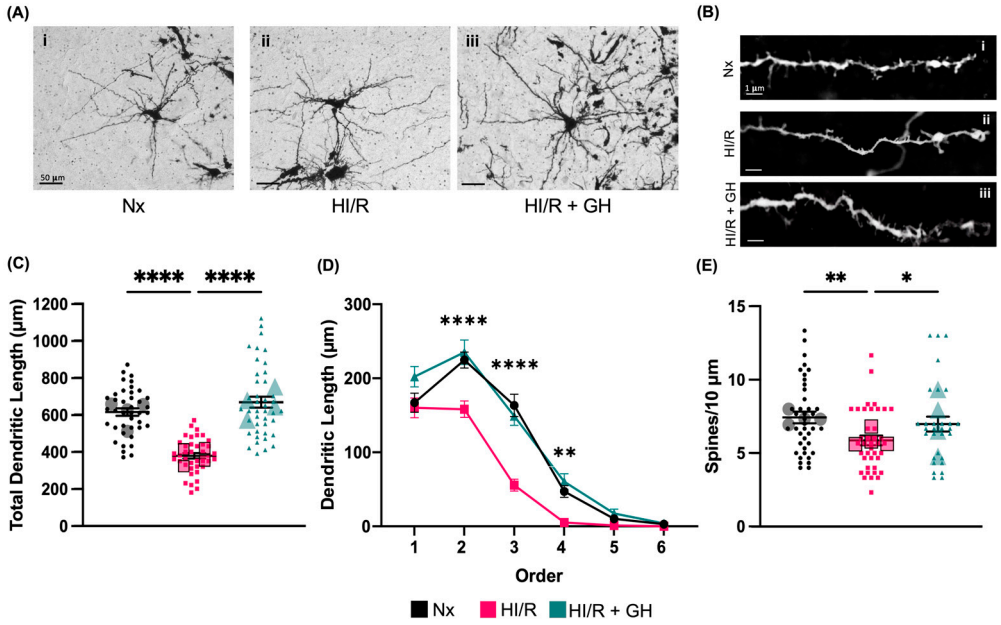


Figure 7. Effect of GH upon structural plasticity after hypoxic-ischemic and reoxygenation (HI/R) injury. (**A**) Representative images of pallial neurons stained with Golgi of each experimental group: (**i**) normoxia, (**ii**) HI/R and (**iii**) HI/R + GH. Scale bar: 10 µm. (**B**) Representative photomicrographs of dendritic segments from pallial neuron showing Golgi-Cox-stained spines for each experimental group: (**i**) normoxia, (**ii**) HI/R and (**iii**) HI/R + GH. Scale bar: 1 µm. (**C**) For total dendritic length analysis, individual neurons were selected and drawn using a camera lucida at 40× magnification. Dendrites from each pyramidal neuron, including all branches, were quantified using Sholl analysis. (**D**) Branch-order analysis of pallial neurons in each experimental group. (**E**) The number of dendritic spines was estimated in 10 µm segments of each neuron. Small symbols represent individual neurons, and large symbols represent the mean of each embryo (10 neurons per embryo). Horizontal lines represent mean ± SEM; $n = 4$ embryos per group, on which statistical analysis was performed. Asterisks show multiple comparisons among groups, * $p < 0.05$, ** $p < 0.01$, **** $p < 0.0001$, determined by one-way ANOVA with Fisher' protected LSD as post hoc test. For branch-order analysis, a two-way ANOVA, followed by Fisher's LSD test as post hoc test, was applied, ** $p < 0.01$, **** $p < 0.0001$.

4. Discussion

This study shows that GH attenuates oxidative stress in the chicken *pallium* following HI/R injury. Our findings indicate that GH treatment significantly reduced H_2O_2 production in the lesioned cultured pallial neurons, and this effect was associated with a partial recovery of the GSH/GSSG ratio. Consistently, in vivo administration of GH decreased lipid and protein oxidation while increasing the activity of endogenous antioxidant enzymes, including SOD and CAT. At the transcriptional level, GH selectively modulated antioxidant gene expression after HI/R injury, restoring *Gpx* and *Nrf2* mRNA levels to near control values. In contrast, *Cat* expression decreased with GH treatment, whereas *Sod1* and *Sod2* expression remained unchanged. These molecular effects were accompanied by the regulation of AIF and HIF-1α protein expression. Importantly, the antioxidant actions of GH were accompanied by structural preservation, as GH promoted structural plasticity in HI/R-injured hyperpallium neurons, restoring total dendritic length and branching complexity. Furthermore, the marked reduction in dendritic spine density induced by HI/R was partially reversed by GH treatment. Together, these findings indicate that GH not only mitigates oxidative stress but also preserves neuronal architecture,

suggesting that its neuroprotective effects encompass both redox balance and structural modulatory mechanisms.

Therapeutic hypothermia, the standard treatment for HIE, reduces mortality and improves some neurological outcomes in full-term neonates [40]; however, a notable proportion of treated infants still develop cerebral palsy or cognitive impairments [40,41], and this treatment is not recommended for preterm infants [42]. Consequently, adjuvant neuroprotective strategies, such as erythropoietin, melatonin, insulin-like growth factor 1 (IGF-1) and stem cells, are being investigated [42–46]. GH is an attractive candidate because it promotes neuronal survival, the proliferation and differentiation of neural precursors, neurite outgrowth and synaptogenesis [31,47–50]. Furthermore, its therapeutic potential has been evaluated in patients with brain injury [51,52]. Also, it was able to cross the blood–brain barrier and promote protective and restorative processes in the chick embryo brain after prenatal HI injury [28–33]. The chick embryo model allows the study of prenatal hypoxic injury and the administration of treatments through the allantoic sac without maternal or placental influences [28–33].

4.1. GH Reduces H_2O_2 and Preserves GSH in Pallial Cell Cultures

In pallial cultures, representative CellROX images suggested that HI/R increased intracellular ROS and that GH attenuated such rise. However, fluorescence imaging was interpreted primarily as a qualitative indicator because a single representative field per condition was examined and the signal of fluorescent probes can be influenced by probe loading efficiency, intracellular enzymatic activity, photobleaching, non-specific oxidation by multiple reactive species, and cell density [53,54]. Therefore, our conclusions regarding ROS rely mainly on the quantitative measurement of H_2O_2, which increased significantly after HI/R injury and returned to normoxic levels with GH treatment, supporting the capacity of GH to mitigate oxidative stress. The mechanism through which GH reduces ROS formation is unclear but could be associated with its ability to regulate NMDA receptors, as previously described in the neural retina exposed to kainate-induced excitotoxic damage [55]. The activation of NMDA receptors is involved in the primary response to HI insult, leading to increased ROS production through NO and NOX2 activation [14]. However, this possibility was not addressed in the present study.

The reduction in ROS levels after GH could also be linked to the regulation of the endogenous glutathione system, which is activated by cells in response to oxidative stress [56]. HI/R injury reduced total and reduced GSH levels, which were associated with an increase in GSSG levels. These findings are consistent with previous studies describing a depletion of endogenous GSH in the immature brain following HI injury [57]. GH preserved GSH levels, whereas the GSH/GSSG ratio showed a partial recovery and remained below normoxic values, indicating that redox balance was not fully restored. Because GH increased GSH without lowering GSSG, this effect is probably more related to increased GSH synthesis or reduced GSH consumption than to an enhanced regeneration of GSH from GSSG, a reaction catalyzed by glutathione reductase rather than by glutathione peroxidase (GPx), which consumes GSH to detoxify peroxides [58]. As neither GSH synthesis nor glutathione reductase activity was assessed, the underlying mechanism remains to be determined. Moreover, the full normalization of H_2O_2 levels contrasted with the partial recovery of the GSH/GSSG ratio, suggesting that glutathione-independent mechanisms may also contribute to H_2O_2 removal in GH-treated cultures.

4.2. GH Reduces Oxidative Damage and Enhances Antioxidant Enzyme Activities In Vivo

The fetal brain is especially vulnerable to oxidative damage due to its high PUFA in membrane phospholipids [59]. We estimated the effect of GH treatment upon lipid peroxidation with a TBARS assay, expressed as MDA equivalents [60]. Because thiobarbituric acid also reacts with other aldehydes and sample components, this assay provides an index of lipid peroxidation rather than a specific measurement of MDA. HI/R injury increased TBARS levels in the pallium, consistent with previous reports in the cerebellum of chick embryos [30] and in peripheral fetal tissues exposed to hypoxia [61]. Given that MDA is involved in secondary deleterious reactions, including DNA damage, mutagenesis, and apoptosis [62,63], its elevation reflects oxidative stress and may further exacerbate cellular damage. Interestingly, GH treatment decreased MDA levels after HI/R injury to values similar to those of the normoxic control, as previously reported in the cerebellum of chick embryos exposed to hypoxia [31].

Protein carbonylation disrupts the function of multiple proteins and contributes to oxidative stress-induced cellular damage by disrupting redox homeostasis and altering cell cycle regulation, ultimately contributing to cell death [64–66], in part by increasing susceptibility to apoptotic triggers like calpains [64]. Clinically, elevated protein carbonyl levels have been reported in umbilical cord blood from neonates exposed to perinatal hypoxia [67], and their quantification is considered a gold-standard marker of protein oxidation [68]. In agreement with these observations, HI/R injury significantly increased protein carbonyl content in the cerebral *pallium*, and GH reversed this effect. As with TBARS, the DNPH-based carbonyl assay is not entirely specific, since other compounds, such as nucleic acids, may contribute to the signal; therefore, both measurements should be considered complementary indicators of oxidative damage.

Although the mechanism by which GH prevents lipid and protein oxidation remains unclear, it may involve the enhancement of endogenous antioxidant defenses. HI/R reduced SOD activity, which was partially restored by GH, whereas GH increased CAT activity above normoxic levels. Together with the preservation of GSH observed in GH-treated cultures, these changes suggest that GH reinforces several components of the endogenous antioxidant defense, which may contribute to limiting ROS accumulation and oxidative damage to lipids and proteins.

4.3. GH Selectively Modulates Antioxidant Gene Expression

One plausible pathway underlying these GH effects involves the activation of NRF2, a master regulator of redox homeostasis that controls the transcription of multiple antioxidant genes [69]. To explore this possibility, we evaluated the expression of key antioxidant genes—*Sod1*, *Sod2*, *Cat*, *Gpx* and *Nrf2*. Our results indicate that GH modulates antioxidant genes selectively rather than producing generalized activation of redox pathways. HI/R exposure reduced *Gpx*, *Nrf2* and *Sod2* mRNA levels, whereas *Cat* showed a non-significant tendency to increase, and *Sod1* was not significantly changed in comparison to the normoxic control. This pattern agrees with previous studies demonstrating that HI injury alters redox regulation in the immature brain through differential modulation of antioxidant genes [70,71]. Interestingly, *Cat* mRNA expression showed a tendency to increase following HI/R injury, while CAT enzymatic activity was significantly reduced. This discrepancy may reflect compensatory transcriptional upregulation in response to oxidative stress, together with inactivation of the enzyme. Conversely, GH reduced *Cat* mRNA levels despite restoring CAT activity; since catalase upregulation is a secondary adaptive mechanism under oxidative stress [72], this normalization may indicate restoration of redox equilibrium rather than suppression of antioxidant defense.

One of the most relevant findings is the restoration of *Gpx* expression by GH treatment. GPx reduces H_2O_2 and lipid hydroperoxides at the expense of GSH [73], particularly

during reoxigenation, when ROS generation increases [34], and reduced GPx activity has been associated with enhanced lipid peroxidation after neonatal HI [71]. Therefore, the restoration of *Gpx* expression is consistent with the lower lipid peroxidation observed in GH-treated embryos, although GPx protein levels and activity were not measured.

NRF2 controls the transcription of *Sod1/2*, *Cat* and *Gpx* [74]. Neurons deficient in NRF2 are more vulnerable to oxidative stress [75,76], and its genetic deletion exacerbates ischemic brain injury, while pharmacological or genetic activation reduces tissue damage [77,78], and impaired NRF2 activation has been associated with insufficient endogenous antioxidant responses after neonatal HI [79]. In our model, HI/R reduced *Nrf2* expression, and GH restored it to normoxic levels. NRF2 activity can be regulated by JAK/STAT signaling and by hormones such as prolactin [21], and GH acts through JAK2/STAT signaling in the developing and adult nervous system [80–83]; thus, GH-induced JAK2/STAT signaling might contribute to the preservation of NRF2-dependent responses. However, since only mRNA levels were assessed and NRF2 protein levels, nuclear translocation and ARE-dependent transcriptional activity were not evaluated, further studies are required to determine whether GH directly activates this pathway or indirectly preserves it by attenuating oxidative stress.

4.4. GH Effects on AIF and HIF-1α

HI/R produced only a non-significant tendency to increase AIF-IR in the pallial tissue ($p = 0.06$), whereas AIF-IR in GH-treated embryos was significantly lower than in the HI/R group and comparable to controls. Although apoptosis was not directly quantified in the present study, this finding is compatible with an attenuation of AIF-dependent cell death pathways by GH, in line with the anti-apoptotic effects in cerebellar and hippocampal neurons following HI injury [29,32]. However, total AIF abundance does not by itself indicate AIF-mediated cell death, which requires its mitochondrial release and nuclear translocation [84,85].

HIF-1α is a key regulator of the molecular response to hypoxia [86]. In the present study, HI/R produced a modest increase in HIF-1α-IR (approximately 9%), consistent with persistent hypoxia signaling during reoxygenation, whereas GH reduced HIF-1α-IR below normoxic levels. Because HIF-1α also drives adaptive responses that support neural survival, such as the induction of erythropoietin, vascular endothelial growth factor and glycolytic enzymes [87], a reduction below basal levels should not be assumed to be beneficial, and its functional consequences remain to be determined. A possible explanation involves the effect of GH on NO production, a recognized initiator of ROS generation during HI events [88], since NO can stabilize HIF-1α through the activation of PI3K/AKT and MAPK pathways [89–91], and GH reduces NO production and activates these pathways) in the cerebellum of chick embryos exposed to HI insult [29,30].

4.5. GH Preserves Structural Plasticity

Beyond its antioxidant effects, GH preserved the dendritic structure of hyperpallium neurons after HI/R injury. HI injury disrupts dendritic architecture and synaptic organization [31,32,92], and excessive ROS alter cytoskeletal polymerization, destabilize microtubules and impair synaptic protein function, promoting dendritic retraction and spine loss [93,94]. Accordingly, HI/R reduced dendritic length, dendritic branching, and spine density, consistent with the dendritic retraction, cytoskeletal destabilization, and spine loss after neonatal HI [95,96]. Importantly, GH restored total dendritic length to values comparable to those of normoxic controls. The loss of dendritic length after HI/R was most evident at the second to fourth branch orders, suggesting that GH preserves intermediate and distal dendritic segments, which are particularly susceptible to oxidative damage and glutamate-mediated excitotoxicity [97,98]. GH also attenuated the loss of dendritic spines,

which results from ROS accumulation, NMDA receptor overactivation, calcium overload and cytoskeletal breakdown [93,97].

The concurrent improvement of redox markers and neuronal morphology suggests that both effects may be linked, for instance, through NRF2-dependent responses, whose activation preserves dendritic architecture and synaptic proteins under oxidative and ischemic conditions [79,99], as well as with the participation of PI3K/Akt and MAPK/ERK pathways, which are involved in neuronal growth and synaptic plasticity [32,82], promote cytoskeletal stabilization and dendritic growth [100] and contribute to spine formation and synaptic strengthening [101]. These pathways are activated by GH [32,82], as we have previously shown in embryonic chicken and early postnatal rat models of hypoxic injury [31–33]. However, this association should be interpreted as a potential link rather than as a cause-and-effect relationship. Future studies will be required to determine whether GH-induced redox stabilization and structural remodeling converge through modulation of these pathways.

4.6. Limitations

First, the term HI/R, retained for consistency with our previous studies using the same paradigms [28,29,32], applies differently to each model: the in vitro paradigm combines reduced oxygen and glucose availability, which mimics some features of ischemia, whereas the in vivo paradigm consists of systemic hypoxia, followed by reoxygenation, without direct manipulation or measurement of cerebral blood flow; therefore, an ischemic component of the in vivo injury was not demonstrated. Second, all analyses were performed at a single time point after reoxygenation, and morphological analyses were restricted to the hyperpallium. Third, GH was administered at the onset of hypoxia, a prophylactic regimen that differs from the clinical situation, in which treatment can only begin after the insult. Finally, although the chick embryo allows the study of prenatal injury without maternal or placental influences, differences in brain development and physiology between birds and mammals limit the direct translation of these findings to the human neonate.

5. Conclusions

Our results indicate that GH acts as a modulator of oxidative stress in an embryonic HI/R injury model, both in vitro and in vivo. GH attenuated ROS production, reduced lipid and protein oxidation, enhanced endogenous antioxidant responses, and reduced AIF and HIF-1α protein levels. Importantly, these molecular effects were accompanied by the preservation of dendritic morphology and spine density, suggesting that GH preserves structural plasticity under injurious conditions. Collectively, these results identify GH as a modulator of redox balance and neuronal structural integrity following prenatal hypoxic-ischemic injury and provide a rationale for further mechanistic and translational studies of GH-mediated neuroprotection.

Supplementary Materials: The following supporting information can be downloaded at: https://www.mdpi.com/article/10.3390/cimb48111219/s1.

Author Contributions: Conceptualization, J.D.O.-H. and C.A.; Methodology: J.D.O.-H., M.C., V.A.U.-S. and J.E.B.-M.; Supervision: C.A., J.D.O.-H., C.G.M.-M., M.L. and J.Á.-M.; Writing—original draft, J.D.O.-H. and C.A.; Writing—review and editing, C.A., J.D.O.-H., C.G.M.-M., M.L. and J.Á.-M.; Resources and funding, C.A., M.L., J.Á.-M. and C.G.M.-M. All authors have read and agreed to the published version of the manuscript.

Funding: This work was supported by grants IN207524, IN209124, IN218325, IN215522, IA200622, and IN227020 from Programa de Apoyo a Proyectos de Investigación e Innovación Tecnológica de

la Dirección General de Asuntos del Personal Académico, Universidad Nacional Autónoma de México (PAPIIT-DGAPA-UNAM, Mexico City, Mexico), and UNAM grant 1130-202-002 to C.A.; as well as by grant 214971 from Consejo Nacional de Humanidades, Ciencia y Tecnología (CONAHCYT, Mexico City, Mexico) and grant CBF-2025-G-1038 from Secretaría de Ciencia, Humanidades, Tecnología e Innovación (SECIHTI, Mexico City, Mexico). Postdoctoral fellowship to J.D.O.-H was provided by Fondo Alejandro Bayón (2021–2022), sponsored by C.A.; Ph.D. scholarships to V.A.U-S. (# 787975) and J.E.B-M. (# 921788) were provided by CONAHCYT and Fondo Alejandro Bayón (2023–2026).

Institutional Review Board Statement: This study was conducted according to the guidelines established in "The guide for care and use of laboratory animals", U.S. National Research Council, as well as in the Mexican official regulation (NOM-062-ZOO-1999), and were approved by the Institute of Neurobiology Research Ethics Committee (protocol 038, 19 October 2010, ratified on 12 September 2017).

Informed Consent Statement: Not applicable.

Data Availability Statement: The data that support the findings of this study are available from the corresponding author upon reasonable request.

Acknowledgments: The authors thank Pilgrim's Pride, Querétaro, México, who donated fertilized broiler eggs used during this research. We also thank Gerardo Courtois (Lab assistant), Nydia Hernández-Ríos, at the Microscopy Unit; Adriana González-Gallardo, at the Proteogenomic Unit; Ramón Martínez-Olvera and Omar González-Hernández, at the Information and Communication Technologies Unit, all from INB-UNAM, for technical support. We express our gratitude to Mauricio Díaz-Muñoz for critically reading the manuscript and valuable comments. We also thank Enrique Juárez Aguilar (Universidad Veracruzana) for granting access to his microscope, which was essential for neuronal reconstruction and morphological analysis.

Conflicts of Interest: The authors declare no conflicts of interest.

References

1. Novak, C.M.; Ozen, M.; Burd, I. Perinatal brain injury: Mechanisms, prevention, and outcomes. *Clin. Perinatol.* **2018**, *45*, 357–375.
2. Greco, P.; Nencini, G.; Piva, I.; Scioscia, M.; Volta, C.A.; Spadaro, S.; Neri, M.; Bonaccorsi, G.; Greco, F.; Cocco, I.; et al. Pathophysiology of hypoxic-ischemic encephalopathy: A review of the past and a view on the future. *Acta Neurol. Belg.* **2020**, *120*, 277–288.
3. Molloy, E.J.; El-Dib, M.; Juul, S.E.; Benders, M.; Gonzalez, F.; Bearer, C.; Wu, Y.W.; Robertson, N.J.; Hurley, T.; Branagan, A.; et al. Neuroprotective Therapies in the NICU in Term Infants: Present and Future. *Pediatr. Res.* **2023**, *93*, 1819–1827.
4. Zhang, X.; Peng, K.; Zhang, X. The function of the NMDA receptor in hypoxic-ischemic encephalopathy. *Front. Neurosci.* **2020**, *14*, 567665.
5. Chen, Y.; Li, X.; Xiong, Q.; Du, Y.; Luo, M.; Yi, L.; Pang, Y.; Shi, X.; Wang, Y.T.; Dong, Z. Inhibiting NLRP3 inflammasome signaling pathway promotes neurological recovery following hypoxic-ischemic brain damage by increasing p97-mediated surface GluA1-containing AMPA receptors. *J. Transl. Med*. **2023**, *21*, 567.
6. Si, W.; Li, B.; Lenahan, C.; Li, S.; Gu, R.; Qu, H.; Wang, L.; Liu, J.; Tian, T.; Wang, Q.; et al. AT1R/GSK-3β/mTOR signaling pathway involved in angiotensin II-induced neuronal apoptosis after HIE both in vitro and in vivo. *Oxid. Med. Cell Longev.* **2020**, *2020*, 8864323.
7. Ye, L.; Feng, Z.; Doycheva, D.; Malaguit, J.; Dixon, B.; Xu, N.; Zhang, J.H.; Tang, J. CpG-ODN exerts a neuroprotective effect via the TLR9/pAMPK signaling pathway by activation of autophagy in a neonatal HIE rat model. *Exp. Neurol*. **2018**, *301*, 70–80.
8. Zhao, J.; Le, M.; Li, J.; Huang, Q.; Chen, H.; Zhang, W.; Mao, H.; Sun, Q.; Li, A.; Zhao, Y.; et al. LINC00938 alleviates hypoxia ischemia encephalopathy induced neonatal brain injury by regulating oxidative stress and inhibiting JNK/p38 MAPK signaling pathway. *Exp. Neurol.* **2023**, *367*, 114449.
9. Salim, S. Oxidative stress and the central nervous system. *J. Pharmacol. Exp. Ther.* **2017**, *360*, 201–205.

10. Tan, S.; Zhou, F.; Nielsen, V.G.; Wang, Z.; Gladson, C.L.; Parks, D.A. Sustained hypoxia-ischemia results in reactive nitrogen and oxygen species production and injury in the premature fetal rabbit brain. *J. Neuropatho. Exp. Neurol.* **1998**, *57*, 544–553.
11. Torres-Cuevas, I.; Corral-Debrinski, M.; Gressens, P. Brain oxidative damage in murine models of neonatal hypoxia/ischemia and reoxygenation. *Free Radic. Biol. Med.* **2019**, *142*, 3–15.
12. Murphy, M.P.; Bayir, H.; Belousov, V.; Chang, C.J.; Davies, K.J.A.; Davies, M.J.; Dick, T.P.; Finkel, T.; Forman, H.J.; Janssen-Heininger, Y.; et al. Guidelines for measuring reactive oxygen species and oxidative damage in cells and in vivo. *Nat. Metab.* **2022**, *4*, 651–662.
13. Covarrubias, L.; Hernández-García, D.; Schnabel, D.; Salas-Vidal, E.; Castro-Obregón, S. Function of reactive oxygen species during animal development: Passive or active? *Dev. Biol.* **2008**, *320*, 1–11.
14. Girouard, H.; Wang, G.; Gallo, E.F.; Anrather, J.; Zhou, P.; Pickel, V.M.; Iadecola, C. NMDA receptor activation increases free radical production through nitric oxide and NOX2. *J. Neurosci.* **2009**, *29*, 2545–2552.
15. Yan, L.L.; Zaher, H.S. How do cells cope with RNA damage and its consequences? *J. Biol. Chem.* **2019**, *294*, 15158–15171.
16. Juan, C.A.; Pérez de la Lastra, J.M.; Plou, F.J.; Pérez-Lebeña, E. The chemistry of reactive oxygen species (ROS) revisited: Outlining their role in biological macromolecules (DNA, lipids and proteins) and induced pathologies. *Int. J. Mol. Sci.* **2021**, *22*, 4642.
17. Ito, F.; Sono, Y.; Ito, T. Measurement and clinical significance of lipid peroxidation as a biomarker of oxidative stress: Oxidative stress in diabetes, atherosclerosis, and chronic inflammation. *Antioxidants* **2019**, *8*, 72.
18. Hawkins, C.L.; Davies, M.J. Detection, identification, and quantification of oxidative protein modifications. *J. Biol. Chem.* **2019**, *294*, 19683–19708.
19. Iwata, E.; Asanuma, M.; Nishibayashi, S.; Kondo, Y.; Ogawa, N. Different effects of oxidative stress on activation of transcription factors in primary cultured rat neuronal and glial cells. *Brain Res. Mol. Brain Res.* **1997**, *50*, 213–220.
20. Lim, J.L.; van der Pol, S.M.; Baron, W.; McCord, J.M.; de Vries, H.E.; van Horssen, J. Protandim protects oligodendrocytes against an oxidative insult. *Antioxidants* **2016**, *5*, 30.
21. Ulloa, M.; Macías, F.; Clapp, C.; Martínez de la Escalera, G.; Arnold, E. Prolactin is an endogenous antioxidant factor in astrocytes that limits oxidative stress-induced astrocytic cell death via the STAT3/NRF2 signaling pathway. *Neurochem. Res.* **2024**, *49*, 1879–1901.
22. Ávila-Mendoza, J.; Mora, J.; Carranza, M.; Luna, M.; Arámburo, C. Growth hormone reverses excitotoxic damage induced by kainic acid in the green iguana neuroretina. *Gen. Comp. Endocrinol.* **2016**, *234*, 57–67.
23. Sanchez-Bezanilla, S.; Åberg, N.D.; Crock, P.; Walker, F.R.; Nilsson, M.; Isgaard, J.; Ong, L.K. Growth Hormone promotes motor function after experimental stroke and enhances recovery-promoting mechanisms within the peri-infarct area. *Int. J. Mol. Sci.* **2020**, *21*, 606.
24. Sanchez-Bezanilla, S.; Åberg, N.D.; Crock, P.; Walker, F.R.; Nilsson, M.; Isgaard, J.; Ong, L.K. Growth hormone treatment promotes remote hippocampal plasticity after experimental cortical stroke. *Int. J. Mol. Sci.* **2020**, *21*, 4563.
25. Martínez-Moreno, C.G.; Fleming, T.; Carranza, M.; Ávila-Mendoza, J.; Luna, M.; Harvey, S.; Arámburo, C. Growth hormone protects against kainate excitotoxicity and induces BDNF and NT3 expression in chicken neuroretinal cells. *Exp. Eye Res.* **2018**, *166*, 1–12.
26. Martínez-Moreno, C.G.; Calderón-Vallejo, D.; Díaz-Galindo, C.; Hernández-Jasso, I.; Olivares-Hernández, J.D.; Ávila-Mendoza, J.; Epardo, D.; Balderas-Márquez, J.E.; Urban-Sosa, V.A.; Baltazar-Lara, R.; et al. Gonadotropin-releasing hormone and growth hormone act as anti-inflammatory factors improving sensory recovery in female rats with thoracic spinal cord injury. *Front. Neurosci.* **2023**, *17*, 1164044.
27. Martínez-Moreno, C.G.; Calderón-Vallejo, D.; Díaz-Galindo, C.; Hernández-Jasso, I.; Olivares-Hernández, J.D.; Ávila-Mendoza, J.; Epardo, D.; Balderas-Márquez, J.E.; Urban-Sosa, V.A.; Baltazar-Lara, R.; et al. Neurotrophic and synaptic effects of GnRH and/or GH upon motor function after spinal cord injury in rats. *Sci. Rep.* **2024**, *14*, 26420.
28. Alba-Betancourt, C.; Luna-Acosta, J.L.; Ramírez-Martínez, C.E.; Avila-González, D.; Granados-Ávalos, E.; Carranza, M.; Martínez-Coria, H.; Arámburo, C.; Luna, M. Neuroprotective effects of growth hormone (GH) after hypoxia-ischemia injury in embryonic chicken cerebellum. *Gen. Comp. Endocrinol.* **2013**, *183*, 17–31.
29. Baltazar-Lara, R.; Ávila-Mendoza, J.; Martínez-Moreno, C.G.; Carranza, M.; Pech-Pool, S.; Vázquez-Martínez, O.; Díaz-Muñoz, M.; Luna, M.; Arámburo, C. Neuroprotective effects of growth hormone (GH) and insulin-like growth factor type 1 (IGF-1) after hypoxic-ischemic injury in chicken cerebellar cell cultures. *Int. J. Mol. Sci.* **2020**, *22*, 256.
30. Olivares-Hernández, J.D.; Balderas-Márquez, J.E.; Carranza, M.; Luna, M.; Martínez-Moreno, C.G.; Arámburo, C. Growth hormone (GH) enhances endogenous mechanisms of neuroprotection and neuroplasticity after oxygen and glucose deprivation injury (OGD) and reoxygenation (OGD/R) in chicken hippocampal cell cultures. *Neural Plast.* **2021**, *2021*, 9990166.

31. Baltazar-Lara, R.; Zenil, J.M.; Carranza, M.; Ávila-Mendoza, J.; Martínez-Moreno, C.G.; Arámburo, C.; Luna, M. Growth hormone (GH) crosses the blood-brain barrier (BBB) and induces neuroprotective effects in the embryonic chicken cerebellum after a hypoxic injury. *Int. J. Mol. Sci.* **2022**, *23*, 11546.
32. Olivares-Hernández, J.D.; Carranza, M.; Balderas-Márquez, J.E.; Epardo, D.; Baltazar-Lara, R.; Ávila-Mendoza, J.; Martínez-Moreno, C.G.; Luna, M.; Arámburo, C. Neuroprotective and regenerative effects of growth hormone (GH) in the embryonic chicken cerebral pallium exposed to hypoxic-ischemic (HI) injury. *Int. J. Mol. Sci.* **2022**, *23*, 9054.
33. Baltazar-Lara, R.; Carranza, M.; Martínez-Moreno, C.G.; Ávila-Mendoza, J.; Arámburo, C.; Luna, M. Growth hormone effects on hypoxia-induced neuroinflammation in the developing cerebellum. *Int. J. Mol. Sci.* **2025**, *26*, 10671.
34. Coimbra-Costa, D.; Alva, N.; Duran, M.; Carbonell, T.; Rama, R. Oxidative stress and apoptosis after acute respiratory hypoxia and reoxygenation in rat brain. *Redox Biol.* **2017**, *12*, 216–225.
35. Livak, K.J.; Schmittgen, T.D. Analysis of relative gene expression data using real-time quantitative PCR and the 2 (-Delta Delta C(T)) method. *Methods*. **2001**, *408*, 402–408.
36. Vandesompele, J.; De Preter, K.; Pattyn, F.; Poppe, B.; Van Roy, N.; De Paepe, A.; Speleman, F. Accurate normalization of real-time quantitative RT-PCR data by geometric averaging of multiple internal control genes. *Genome Biol*. **2002**, *3*, research0034.
37. Bas, A.; Forsberg, G.; Hammarström, S.; Hammarström, M.L. Utility of the housekeeping genes 18S rRNA, β-actin and glyceraldehyde-3-phosphate-dehydrogenase for normalization in real-time quantitative reverse transcriptase-polymerase chain reaction analysis of gene expression in human T lymphocytes. *Scand. J. Immunol*. **2004**, *59*, 566–573.
38. Kuenzel, W.J.; Masson, M. *A stereotaxic atlas of the Brain of the Chick (Gallus domesticus)*, 1st ed.; The Johns Hopkins University Press: Baltimore, MD, USA, 1988; 152p.
39. Sholl, D.A. Dendritic organization in the neurons of the visual and motor cortices of the cat. *J. Anat.* **1953**, *87*, 387–406.
40. Davidson, J.O.; Wassink, G.; van den Heuij, L.G.; Bennet, L.; Gunn, A.J. Therapeutic hypothermia for neonatal hypoxic-ischemic encephalopathy—Where to from here? *Front. Neurol.* **2015**, *6*, 198.
41. Arteaga, O.; Álvarez, A.; Revuelta, M.; Santaolalla, F.; Urtasun, A.; Hilario, E. Role of antioxidants in neonatal hypoxic-ischemic brain injury: New therapeutic approaches. *Int. J. Mol. Sci.* **2017**, *18*, 265.
42. Maïza, A.; Hamoudi, R.; Mabondzo, A. Targeting the multiple complex processes of hypoxia-ischemia to achieve neuroprotection. *Int. J. Mol. Sci.* **2024**, *25*, 5449.
43. Lin, S.; Rhodes, P.G.; Cai, Z. Whole body hypothermia broadens the therapeutic window of intranasally administered IGF-1 in a neonatal rat model of cerebral hypoxia-ischemia. *Brain Res.* **2011**, *1385*, 246–256.
44. Ahmad, Q.M.; Chishti, A.L.; Waseem, N. Role of melatonin in management of hypoxic ischaemic encephalopathy in newborns: A randomized control trial. *JPMA J. Pak. Med. Assoc.* **2018**, *68*, 1233–1237.
45. Oorschot, D.E.; Sizemore, R.J.; Amer, A.R. Treatment of neonatal hypoxic-ischemic encephalopathy with erythropoietin alone, and erythropoietin combined with hypothermia: History, current status, and future research. *Int. J. Mol. Sci.* **2020**, *21*, 1487.
46. Teo, E.J.; Jones, L.E.; Wixey, J.A.; Boyd, R.N.; Colditz, P.B.; Bjorkman, S.T. Combined hypothermia and mesenchymal stem cells in animal models of neonatal hypoxic-ischaemic encephalopathy: A systematic review. *Pediatr. Res.* **2022**, *92*, 25–31.
47. Ajo, R.; Cacicedo, L.; Navarro, C.; Sánchez-Franco, F. Growth hormone action on proliferation and differentiation of cerebral cortical cells from fetal rat. *Endocrinology* **2003**, *144*, 1086–1097.
48. Blackmore, D.G.; Reynolds, B.A.; Golmohammadi, M.G.; Large, B.; Aguilar, R.M.; Haro, L.; Waters, M.J.; Rietze, R.L. Growth hormone responsive neural precursor cells reside within the adult mammalian brain. *Sci. Rep.* **2012**, *2*, 250.
49. Regalado-Santiago, C.; López-Meraz, M.L.; Santiago-García, J.; Fernández-Pomares, C.; Juárez-Aguilar, E. Growth hormone (GH) is a survival rather than a proliferative factor for embryonic striatal neural precursor cells. *Growth Horm IGF Res.* **2013**, *23*, 179–186.
50. Nylander, E.; Zelleroth, S.; Stam, F.; Nyberg, F.; Grönbladh, A.; Hallberg, M. Growth hormone increases dendritic spine density in primary hippocampal cell cultures. *Growth Horm. IGF Res.* **2020**, *50*, 42–47.
51. Song, J.; Park, K.; Lee, H.; Kim, M. The effect of recombinant human growth hormone therapy in patients with completed stroke: A pilot trial. *Ann. Rehabil. Med.* **2012**, *36*, 447–457.
52. Szarka, N.; Szellar, D.; Kiss, S.; Farkas, N.; Szakacs, Z.; Czigler, A.; Ungvari, Z.; Hegyi, P.; Buki, A.; Toth, P. Effect of growth hormone on neuropsychological outcomes and quality of life of patients with traumatic brain injury: A systematic review. *J. Neurotrauma* **2021**, *38*, 1467–1483.
53. Wardman, P. Fluorescent and luminescent probes for measurement of oxidative and nitrosative species in cells and tissues: Progress, pitfalls, and prospects. *Free Radic. Biol. Med.* **2007**, *43*, 995–1022.

54. Kalyanaraman, B.; Darley-Usmar, V.; Davies, K.J.; Dennery, P.A.; Forman, H.J.; Grisham, M.B.; Mann, G.E.; Moore, K.; Roberts, L.J., 2nd; Ischiropoulos, H. Measuring reactive oxygen and nitrogen species with fluorescent probes: Challenges and limitations. *Free Radic. Biol. Med.* **2012**, *52*, 1–6.
55. Fleming, T.; Martinez-Moreno, C.G.; Carranza, M.; Luna, M.; Harvey, S.; Arámburo, C. Growth hormone promotes synaptogenesis and protects neuroretinal dendrites against kainic acid (KA) induced damage. *Gen. Comp. Endocrinol.* **2018**, *265*, 111–120.
56. Thiel, A.; Weishaupt, A.K.; Nicolai, M.M.; Lossow, K.; Kipp, A.P.; Schwerdtle, T.; Bornhorst, J. Simultaneous quantitation of oxidized and reduced glutathione via LC-MS/MS to study the redox state and drug-mediated modulation in cells, worms and animal tissue. *J. Chromatogr.* **2023**, *1225*, 123742.
57. Wallin, C.; Puka-Sundvall, M.; Hagberg, H.; Weber, S.G.; Sandberg, M. Alterations in glutathione and amino acid concentrations after hypoxia-ischemia in the immature rat brain. *Brain Res. Dev. Brain Res.* **2000**, *125*, 51–60.
58. Saydam, N.; Kirb, A.; Demir, O.; Hazan, E.; Oto, O.; Saydam, O.; Güner, G. Determination of glutathione, glutathione reductase, glutathione peroxidase and glutathione S-transferase levels in human lung cancer tissues. *Cancer Lett.* **1997**, *119*, 13–19.
59. Zaleska, M.M.; Floyd, R.A. Regional lipid peroxidation in rat brain in vitro: Possible role of endogenous iron. *Neurochem. Res.* **1985**, *10*, 397–410.
60. Esterbauer, H.; Schaur, R.J.; Zollner, H. Chemistry and biochemistry of 4-hydroxynonenal, malonaldehyde and related aldehydes. *Free Radic. Biol. Med.* **1991**, *11*, 81–128.
61. Al-Hasan, Y.M.; Evans, L.C.; Pinkas, G.A.; Dabkowski, E.R.; Stanley, W.C.; Thompson, L.P. Chronic hypoxia impairs cytochrome oxidase activity via oxidative stress in selected fetal guinea pig organs. *Reprod. Sci.* **2013**, *20*, 299–307.
62. Niedernhofer, L.J.; Daniels, J.S.; Rouzer, C.A.; Greene, R.E.; Marnett, L.J. Malondialdehyde, a product of lipid peroxidation, is mutagenic in human cells. *J. Biol. Chem.* **2003**, *278*, 31426–31433.
63. Willis, M.S.; Klassen, L.W.; Carlson, D.L.; Brouse, C.F.; Thiele, G.M. Malondialdehyde-acetaldehyde haptenated protein binds macrophage scavenger receptor(s) and induces lysosomal damage. *Int. Immunopharmacol.* **2004**, *4*, 885–899.
64. Oikawa, S.; Yamada, T.; Minohata, T.; Kobayashi, H.; Furukawa, A.; Tada-Oikawa, S.; Hiraku, Y.; Murata, M.; Kikuchi, M.; Yamashima, T. Proteomic identification of carbonylated proteins in the monkey hippocampus after ischemia-reperfusion. *Free Radic. Biol. Med.* **2009**, *46*, 1472–1477.
65. Suzuki, Y.J.; Carini, M.; Butterfield, D.A. Protein carbonylation. *Antioxid. Redox Signal.* **2010**, *12*, 323–325.
66. Dalle-Donne, I.; Rossi, R.; Giustarini, D.; Milzani, A.; Colombo, R. Protein carbonyl groups as biomarkers of oxidative stress. *Clin. Chim. Acta* **2003**, *329*, 23–38.
67. Zitnanová, I.; Sumegová, K.; Simko, M.; Maruniaková, A.; Chovanová, Z.; Chavko, M.; Duracková, Z. Protein carbonyls as a biomarker of fetal-neonatal hypoxic stress. *Clin. Biochem.* **2007**, *40*, 567–570.
68. Davies, M.J.; Fu, S.; Wang, H.; Dean, R.T. Stable markers of oxidant damage to proteins and their application in the study of human disease. *Free Radic. Biol. Med.* **1999**, *27*, 1151–1163.
69. Zhu, H.; Itoh, K.; Yamamoto, M.; Zweier, J.L.; Li, Y. Role of Nrf2 signaling in regulation of antioxidants and phase 2 enzymes in cardiac fibroblasts: Protection against reactive oxygen and nitrogen species-induced cell injury. *FEBS Lett.* **2005**, *579*, 3029–3036.
70. Blomgren, K.; Hagberg, H. Free radicals, mitochondria, and hypoxia-ischemia in the developing brain. *Free Radic. Biol. Med.* **2006**, *40*, 388–397.
71. Vannucci, S.J.; Hagberg, H. Hypoxia-ischemia in the immature brain. *J. Exp. Biol.* **2004**, *207*, 3149–3154.
72. Nandi, A.; Yan, L.J.; Jana, C.K.; Das, N. Role of Catalase in Oxidative Stress- and Age-Associated Degenerative Diseases. *Oxid Med. Cell Longev.* **2019**, *2019*, 9613090.
73. Lubos, E.; Loscalzo, J.; Handy, D.E. Glutathione peroxidase-1 in health and disease: From molecular mechanisms to therapeutic opportunities. *Antioxid. Redox Signal.* **2011**, *15*, 1957–1997.
74. Ma, Q. Role of Nrf2 in oxidative stress and toxicity. *Annu. Rev. Pharmacol. Toxicol.* **2013**, *53*, 401–426.
75. Lee, J.M.; Calkins, M.J.; Chan, K.; Kan, Y.W.; Johnson, J.A. Identification of the NF-E2-related factor-2-dependent genes conferring protection against oxidative stress in primary cortical astrocytes using oligonucleotide microarray analysis. *J. Biol. Chem.* **2003**, *278*, 12029–12038.
76. Lee, J.M.; Shih, A.Y.; Murphy, T.H.; Johnson, J.A. NF-E2-related factor-2 mediates neuroprotection against mitochondrial complex I inhibitors and increased intracellular calcium in primary cortical neurons. *J. Biol. Chem.* **2003**, *278*, 37948–37956.

77. Alfieri, A.; Srivastava, S.; Siow, R.C. M.; Cash, D.; Modo, M.; Duchen, M.R.; Fraser, P.A.; Williams, S.C.R.; Mann, G.E. Sulforaphane preconditioning of the brain protects against transient focal cerebral ischemia in mice via Nrf2-dependent mechanisms. *Free Radic. Biol. Med.* **2013**, *65*, 1012–1022.
78. Liu, M.; Li, W.; Wang, H.; Yin, Y.; Zhu, C.; Zhang, Y. Nrf2 activation attenuates ischemic stroke-induced brain injury via suppression of ferroptosis and oxidative stress. *J. Neurochem.* **2019**, *149*, 140–152.
79. Zhang, W.; Dong, X.; Dou, S.; Yang, L. Neuroprotective role of Nrf2 on hypoxic-ischemic brain injury in neonatal mice. *Synapse* **2020**, *74*, e22174.
80. Arámburo, C.; Alba-Betancourt, C.; Luna, M.; Harvey, S. Expression and function of growth hormone in the nervous system: A brief review. *Gen. Comp. Endocrinol*. **2014**, *203*, 35–42.
81. Bianchi, V.E.; Locatelli, V.; Rizzi, L. Neurotrophic and neuroregenerative effects of GH/IGF1. *Int. J. Mol. Sci.* **2017**, *18*, 2441.
82. Aberg, N.D.; Brywe, K.G.; Isgaard, J. Aspects of growth hormone and insulin-like growth factor-I related to neuroprotection, regeneration, and functional plasticity in the adult brain. *Sci. World J*. **2006**, *6*, 53–80.
83. Arce, V.M.; Devesa, P.; Devesa, J. Role of growth hormone (GH) in the treatment on neural diseases: From neuroprotection to neural repair. *Neurosci. Res.* **2013**, *76*, 179–186.
84. Sevrioukova, I.F. Apoptosis-inducing factor: Structure, function, and redox regulation. *Antioxid. Redox Signal*. **2011**, *14*, 2545–2579.
85. Doti, N.; Reuther, C.; Scognamiglio, P.L.; Dolga, A.M.; Plesnila, N.; Ruvo, M.; Culmsee, C. Inhibition of the AIF/CypA complex protects against intrinsic death pathways induced by oxidative stress. *Cell Death Dis*. **2014**, *5*, e993.
86. Semenza, G.L. Oxygen sensing, hypoxia-inducible factors, and disease pathophysiology. *Annu. Rev. Pathol.* **2014**, *9*, 47–71.
87. Sharp, F.R.; Bernaudin, M. HIF1 and oxygen sensing in the brain. *Nat. Rev. Neurosci.* **2004**, *5*, 437–448.
88. Wierońska, J.M.; Cieślik, P.; Kalinowski, L. Nitric oxide-dependent pathways as critical factors in the consequences and recovery after brain ischemic hypoxia. *Biomolecules* **2021**, *11*, 1097.
89. Brüne, B.; Zhou, J. The role of nitric oxide (NO) in stability regulation of hypoxia inducible factor-1alpha (HIF-1alpha). *Curr. Med. Chem.* **2003**, *10*, 845–855.
90. Brüne, B.; Zhou, J. Hypoxia-inducible factor-1alpha under the control of nitric oxide. *Methods Enzymol*. **2007**, *435*, 463–478.
91. Koshikawa, N.; Hayashi, J.; Nakagawara, A.; Takenaga, K. Reactive oxygen species-generating mitochondrial DNA mutation up-regulates hypoxia-inducible factor-1alpha gene transcription via phosphatidylinositol 3-kinase-Akt/protein kinase C/histone deacetylase pathway. *J. Biol. Chem*. **2009**, *284*, 33185–33194.
92. Cui, C.; Jiang, X.; Wang, Y.; Li, C.; Lin, Z.; Wei, Y.; Ni, Q. Cerebral hypoxia-induced molecular alterations and their impact on the physiology of neurons and dendritic spines: A comprehensive review. *Cell. Mol. Neurobiol.* **2024**, *44*, 58.
93. Wilson, C.; González-Billault, C. Regulation of cytoskeletal dynamics by redox signaling and oxidative stress: Implications for neuronal development and trafficking. *Front. Cell. Neurosci.* **2015**, *9*, 381.
94. Chen, J.; Chen, T.; Wang, Y.; Meng, J.; Tan, G.; Zhao, Q.; Feng, S.; Xu, L.; Pei, Q. Oxidative stress disrupts the cytoskeleton of spinal motor neurons. *Brain Behav.* **2023**, *13*, e2870.
95. McDonald, J.W.; Silverstein, F.S.; Johnston, M.V. Neurotoxicity of N-methyl-D-aspartate is markedly enhanced in developing rat central nervous system. *Brain Res.* **1988**, *459*, 200–203.
96. Zhao, Y.D.; Ou, S.; Cheng, S.Y.; Xiao, Z.; He, W.J.; Zhang, J.H.; Ruan, H.Z. Dendritic development of hippocampal CA1 pyramidal cells in a neonatal hypoxia-ischemia injury model. *J. Neurosci. Res.* **2013**, *91*, 1165–1173.
97. Segal, M. Dendritic spines and long-term plasticity. *Nat. Rev. Neurosci.* **2005**, *6*, 277–284.
98. Katsenos, A.P.; Kotoula, E.; Sereti, S.; Zoidi, D.; Tzavellas, N.P.; Polyzou, A.; Leondaritis, G.; Kanellos, F.S.; Bellou, S.; Bellos, S.; et al. Modeling oxidative stress on neuronal dendrites and dendritic spines. *Neuroscience* **2026**, *592*, 157–166.
99. Kraft, A.D.; Johnson, D.A.; Johnson, J.A. Nuclear factor E2-related factor 2-dependent antioxidant response element activation by tert-butylhydroquinone and sulforaphane occurring preferentially in astrocytes protects neurons against oxidative insult. *J. Neurosci.* **2004**, *24*, 1101–1112.
100. Kumar, V.; Zhang, M.-X.; Swank, M.W.; Kunz, J.; Wu, G.-Y. Regulation of dendritic morphogenesis by Ras–PI3K–Akt–mTOR and Ras–MAPK signaling pathways. *J. Neurosci.* **2005**, *25*, 11288–11299.
101. Thomas, G.M.; Huganir, R.L. MAPK cascade signaling and synaptic plasticity. *Nat. Rev. Neurosci.* **2004**, *5*, 173–183.

Disclaimer/Publisher's Note: The statements, opinions and data contained in all publications are solely those of the individual author(s) and contributor(s) and not of MDPI and/or the editor(s). MDPI and/or the editor(s) disclaim responsibility for any injury to people or property resulting from any ideas, methods, instructions or products referred to in the content.